Int. J. Electrochem. Sci., 15 **(2020)** 2272 – 2280, doi: 10.20964/2020.03.23

International Journal of
ELECTROCHEMICAL
SCIENCE
www.electrochemsci.org

One-step synthesis of needle-like CoO/C composite materials and their enhanced electrochemical performance for supercapacitor

Linna Huang[1,2], Chunyong Zhang[1,2,], Haitao Liu[1,2], Lei Su[1,2], Jianning Li[1,2],Hengfei Qin[2,3,*]*

[1] Jiangsu Key Laboratory of Precious Metal Chemistry and Technology, Jiangsu University of Technology, Changzhou, 213001, China
[2] School of Chemistry and Environmental Engineering, Jiangsu University of Technology, Changzhou, 213001, China
[3] Jiangsu Province Key Laboratory of E-Waste Recycling, Jiangsu University of Technology, Changzhou, 213001, China
Linna Huang, Chunyong Zhang contributed equally to this work and should be considered as co-first authors
[*]E-mail: zhangcy@jsut.edu.cn, jlgqinhf@jsut.edu.cn

Received: 19 October 2019 / *Accepted:* 23 December 2019 / *Published:* 10 February 2020

A needle-like CoO/C composite material was designed to enhance the capacitance performance of CoO via one-step hydrothermal strategy. The obtained CoO/C is applied as electrode material and shows a high specific capacitance, reaching 752 F/g which is outstanding characteristic compared with this of recently reported supercapacitor. The CoO supported on C could provide highly enhanced electrochemical performance and show promising energy storage application. CoO/C can be regarded as promising material for practical supercapacitor and this work also provides a valuable reference for the preparation and application of high performance electrode materials.

Keywords: Supercapacitor; Needle-like; Composite material; One-step

1. INTRODUCTION

Either ion adsorption or fast redox reaction is used in supercapacitor for energy storage [1-2]. Among the available energy storage devices, supercapacitor has high power density and long cycle life, while the energy density is low which limits their application in large-scale energy storage[3]. A growing number of studies are using different electrode materials to increase the properties[4]. In this regard, common electrochemical capacitor electrode materials, such as conductive polymers, metal oxides, and composite electrodes have been demonstrated as promising supercapacitor electrode materials[5].

Cobalt-based materials are good capacitive electrode materials because of their high electrical activity and ease of processing. However, the single cobalt-based materials in supercapacitor are largely hindered by their low electrical conductivity and large volume expansion[6].

Carbon materials such as graphene[7-8], activated carbon[9-10], carbon nanofiber[11-12], carbon nanotube[13-14], templated porous carbon[15-16] and carbidederived carbon[17-18] are well applied in the field of supercapacitor. Biomass carbon material is cheap, environmental friendly and sustainable, which is conductive to the construction of friendly society. Biomass straw was used as carbon material in this study.

In the present work, needle-like CoO/C composite material was constructed by one-step hydrothermal method as electrode material to improve the electrochemical performance of supercapacitor. The structural was characterized by SEM and XRD. The influence of biomass carbon on CoO capacitance was studied by electrochemical test. CoO/C composite material as the electrode material of supercapacitor can improve its specific capacitance and stability, laying a foundation for the commercial application of CoO/C.

2. EXPERIMENTAL

2.1 Chemicals

Ethanol (C_2H_5OH) and Potassium hydroxide (KOH) were obtained from Sinopharm Chemical Reagent Co., Ltd. Polytetrafluoroethylene (5 μm), Acetylene black, Urea ($CO(NH_2)_2$) (≥99%), Nickel nitrate hexahydrate ($Ni(NO_3)_2·6H_2O$) (≥98%) and Cobalt nitrate hexahydrate ($Co(NO_3)_2·6H_2O$) (≥99%) were purchased from Aladdin.

2.2 Materials preparation

Fresh straw (2 cm×1 cm) was cleaned with deionized water and ethanol solution by ultrasonication for 5 min to remove impurities. Under N_2 environment, straw was placed in the steel jade boat, and nitrogen was continuously pumped into the atmosphere tube furnace for 30 min to replace air. The temperature was raised to 650 °C at a rate of 3 °C per minute, and kept for 2 h, and then C was achieved.

In a typical synthetic process, 2 mmol of $Co(NO_3)_2·6H_2O$, 1 mmol of $Ni(NO_3)_2·6H_2O$ and 5 mmol of $CO(NH_2)_2$ were dissolved in 35 mL water by magnetic agitation. The solution prepared above was transferred to the 100 mL stainless steel autoclave. It was kept under the condition of 120 °C for 12 h then naturally cooled to room temperature. The obtained material was washed three times with distilled water and ethanol, and dried at 60 °C for 12 h. After calcinating in tube furnace at 300 °C for 2 h in Nitrogen, $NiCo_2O_4$ was obtained.

In order to synthesize the CoO/C, 2 mmol of $Co(NO_3)_2·6H_2O$, 1 mmol of $Ni(NO_3)_2·6H_2O$ and 5 mmol of $CO(NH_2)_2$ were dissolved in 35 mL water by magnetic agitation. The solution prepared above and C were directly transferred to the 100 mL stainless steel autoclave. It was kept under the condition of 120 °C for 12 h then naturally cooled to room temperature. The obtained material was

washed three times with distilled water and ethanol, and dried at 60 °C for 12 h. Finally the produced materials were calcinated in tube furnace at 300 °C for 2 h in Nitrogen.

2.3 Characterizations

The morphology of CoO/C, C and $NiCo_2O_4$ were observed by scanning electron microscopy (SEM, Hitachi S-3400N). The substance contained in the CoO/C C and $NiCo_2O_4$ were determined by X-ray diffraction (PW3040/60, PANalytical B.V, the scanning range of 2θ is 5-90°). The electrochemical analysis of CoO/C, C and $NiCo_2O_4$ were measured by electrochemical workstation (CHI760E).

2.4 Electrodes preparation

The electrode system was a three-electrode system, with the nickel foam as the working electrodes. Platinum gauze electrode and saturated calomel electrode were used as pair electrodes and reference electrodes respectively.

C, $NiCo_2O_4$ and CoO/C were mixed with PVDF and acetylene black at a mass ratio of 8:1:1 respectively, and 2 mL isopropanol was added as dispersant, which was fully stirred and evenly shaken by ultrasonic shock. The sample was uniformly coated on the pre-treated nickel net with an area of 1 cm×1 cm and dried in a vacuum drying box at 60 °C for 12 h.

The cyclic voltammetry curve was tested by using the three-electrode system prepared above, and the cyclic voltammetry was tested at scanning rates of 0.005, 0.01, 0.02, 0.04 and 0.08 V/s, respectively. According to the cyclic voltammetry curve, the specific capacitance of the electrode was calculated according to following equation, respectively.

$$C_s = \frac{\int IdV}{2m \cdot v \cdot \Delta V}$$

where C_s was the specific capacitance (F/g), I was the current (A), m was the quality of electrode material (g), v was the sweep speed (V/s) and ΔV was the range of voltage (V). The electrochemical impedance spectroscopy was measured under the range from 100 kHz to 0.01 Hz.

3. RESULTS AND DISCUSSION

Due to high specific capacitance and tap cheaply, biomass carbon material has been widely used for electrode materials of supercapacitor. The carbon materials supported CoO have been widely studied, including CoO@GFs (CoO@graphene foams), CoO NB@GF (CoO nanobundles @graphene foams), Co_3O_4 and Co_3O_4/CoO, CoO@NiHON (CoO@nickel hydroxidenitrate nanoflake), CoO/Co_3O_4 and CoO/C. The manifold CoO composite materials mentioned were summarized in Table1.

Table 1. The carbon-based materials supported CoO for supercapacitor

Electrode Material	Electrochemical testing equipment	Test Solutions	Specific capacitance/(F/g)	Reference
CoO@GFs	CHI660B	3 M NaOH	231.87	[19]
CoO NB@GF	CHI660E	3 M NaOH	352.75	[20]
Co_3O_4 and Co_3O_4 /CoO	CHI660D	6 M KOH	362.8	[21]
CoO@NiHON	ZAHNER ZENNIUM	1 M NaOH	798.3	[22]
CoO/Co_3O_4	IVIUMSTAT	3 M KOH	451	[23]
CoO/C	CHI760	6 M KOH	648	[24]
CoO/C	CHI760E	6 M KOH	752	This work

3.1 Construction of $NiCo_2O_4$, C and CoO/C

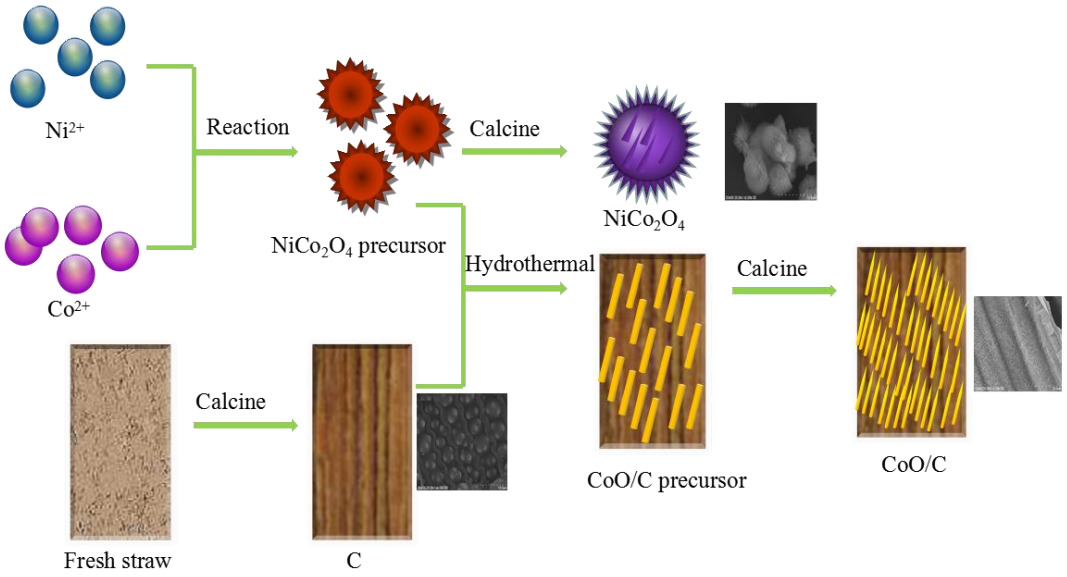

Scheme 1. Schematic diagram of $NiCo_2O_4$ and CoO/C formation process.

As shown in Scheme 1, in order to prepare needle-like CoO/C, C is essential as a carrier. Fig. 1a, b and c show the morphology of $NiCo_2O_4$, C and CoO/C before calcination. Fig. 1d displays the morphologies of $NiCo_2O_4$ and Fig. 1e display the morphologies of C by using carbonized straw. Fig. 1f displays the morphologies of CoO/C with the reduction of the C. Fig. 1d shows a cluster of $NiCo_2O_4$ and a uniform needle of CoO/C in Fig. 1f. Needle of CoO/C provides sufficient accessible channels for ion diffusion within the electrode. Compared with the needle-like object in other article, the specific capacitance of CoO/C is larger[25]. Fig. 1e shows that the carbonized straw presents uniform grain patterns.

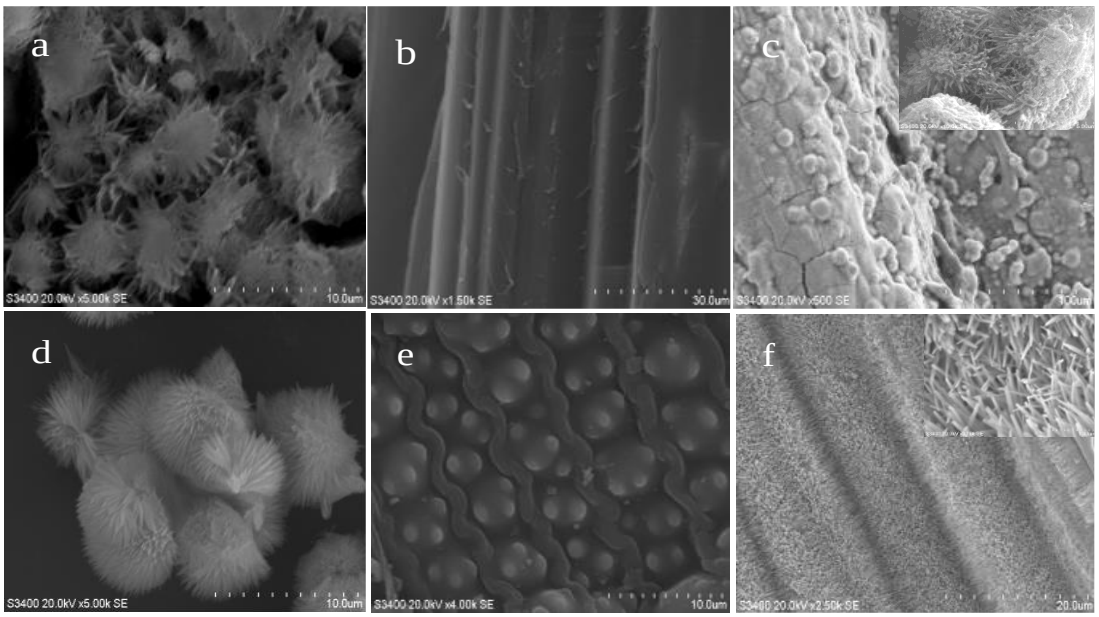

Figure 1. SEM images of (a) $NiCo_2O_4$ precursor, (b) fresh straw, (c) CoO/C precursor, (d) $NiCo_2O_4$, (e) C and (f) CoO/C.

The X-ray diffraction patterns of $NiCo_2O_4$, C and CoO/C can be observed in Fig. 2. The synthesized $NiCo_2O_4$, carbonized straw and CoO/C can be analyzed by XRD to compare the structure of matter. Fig. 2a, b and c show the position of the peak of $NiCo_2O_4$, C and CoO/C before calcination. Fig. 2a shows that $NiCo_2O_4$ is amorphous before calcination, and Fig. 2b and c show peaks of C before calcination.

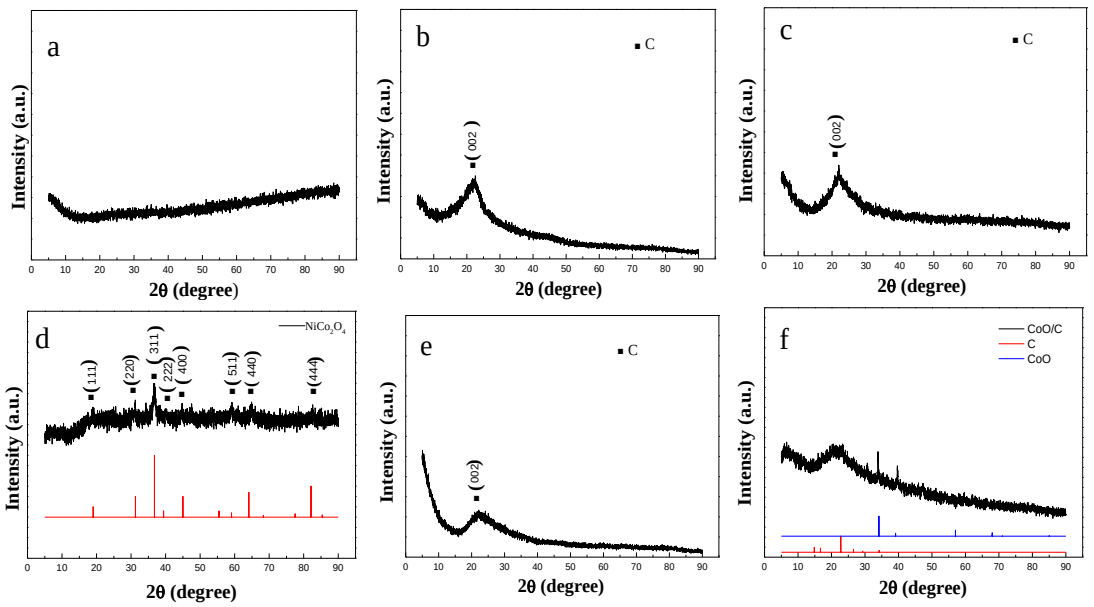

Figure 2. XRD of (a) $NiCo_2O_4$ precursor, (b) fresh straw, (c) CoO/C precursor, (d) $NiCo_2O_4$, (e) C and (f) CoO/C.

As shown in Fig. 2d, peaks of pure $NiCo_2O_4$ are located at 18.9˚, 31.1˚, 36.6˚, 38.4˚, 44.6˚, 59.1˚, 64.8˚and 82.3˚, respectively representing $NiCo_2O_4$ crystal planes of (111), (220), (311), (222), (400), (511), (440) and (444). As shown in Fig. 2e, peaks of carbonized straw are located at 24.7˚, respectively representing carbonized straw crystal planes of (002). As shown in Fig. 2f, peaks of CoO/C are located at 33.9˚and 39.5˚, respectively representing CoO/C crystal planes of (111) and (200).

3.2. Electrochemical characterizations of $NiCo_2O_4$, C and CoO/C.

Electrochemical behaviors of the $NiCo_2O_4$, C and CoO/C were investigated in the electrolyte of 6 M KOH. As shown in the figure below, the cyclic voltammetry curve forms a rectangular shape [26] . In the cyclic voltammetry curves, because of the fast and reversible surface redox reactions of the electrolyte ion in the interface of electrodes, there is no obvious redox peak[27]. CoO/C composite material has a fine needle structure, increasing the contact area with electrolyte, thus reducing the resistivity of the electrode in electrolyte and presenting a better electrical conductivity. From Fig. 3, with the increase of scanning rate, the area of its similar rectangle also increases. Fig. 3d is the comparison diagram of the cyclic volt-ampere curves of $NiCo_2O_4$, C and CoO/C when the scanning rate is 5 mV/s. It can be seen from Fig. 3d that the quasi-rectangular area of CoO/C is the largest, indicating that its capacitance performance is more ideal.

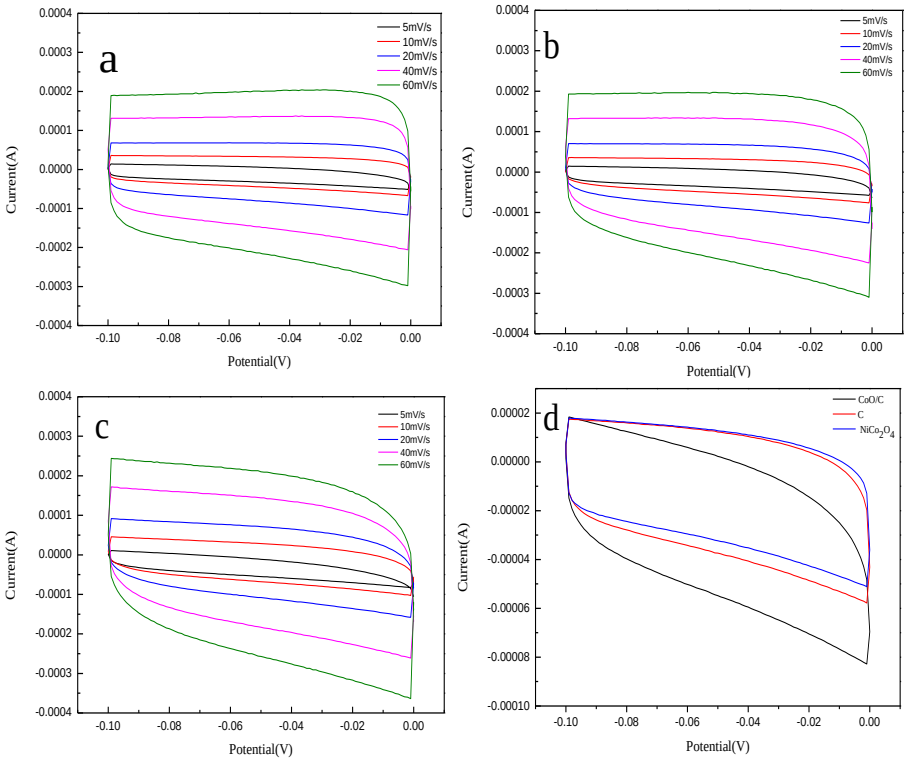

Figure 3. *CVs* of the (a) $NiCo_2O_4$, (b) C, (c) CoO/C electrodes with different scan rates and (d) the comparison at 5 mV/s

CoO/C composite material is needle-like, with larger specific surface area and better stability. In electrochemical experiments, the contact area of CoO/C electrode needle structure with electrolyte increases, thus reducing the electrode resistivity.

Fig. 4 is the constant current charge and discharge curve of 6 M KOH under $NiCo_2O_4$ (a), C (b), CoO/C composite material (c) at different current densities of 1, 2, 3 and 4 A/g. It can be seen from the Fig. 4, with the current density increased, the charge and discharge time of CoO/C composite material as electrode material is the longest. In this paper, the prepared CoO/C composite material has the longest constant-current charge and discharge time, which reflects that the internal resistance is the smallest among the three materials. The corresponding galvanostatic charge-discharge curves reveal voltage plateaus in the charge-discharge process, which is consistent with the CV curves and earlier reports[28]. And the side reflection has a good electrical conductivity, showing more excellent capacitance characteristics.

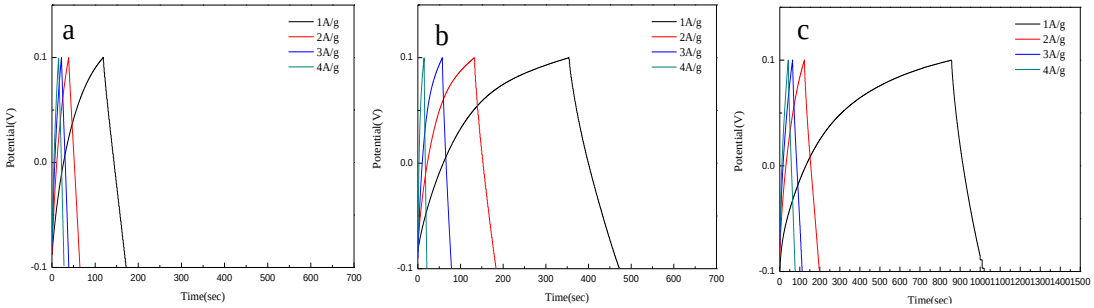

Figure 4. The galvanostatic charge-discharge curves of (a) $NiCo_2O_4$, (b) C and (c) CoO/C in 6 M KOH with different current densities

Fig. 5 shows the specific capacitance (*Csp*) of these three electrodes at different scanning rates in 6 M KOH. The *Csp* measured is shown in Fig. 5. The *Csp* of $NiCo_2O_4$ electrode material is 425 F/g at 5 mV/s. The *Csp* of C of electrode material is 481 F/g at 5 mV/s. The *Csp* of CoO/C composite material is 752 F/g at 5 mV/s. The *Csp* of CoO/C composite is the largest and decreases with the increase of scanning rate. Capacitance retention ability is still very good because of CoO/C composite material in the high current density conditions of long cycle operation.

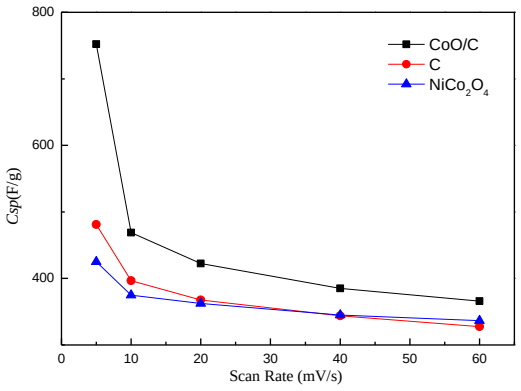

Figure 5. The *Csp* of $NiCo_2O_4$, C and CoO/C in 6 M KOH with different scan rates

Fig. 6 shows the electrochemical impedance spectroscopy of these three electrodes in 6 M KOH. C was introduced to improve the conductivity of CoO/C. In theory, an almost vertical line is the ideal capacitor. According to the figure, in the low-frequency region, the order of impedance arc radius is CoO/C>C>$NiCo_2O_4$. CoO/C material has good capacitance characteristics and good diffusion performance. At high frequencies, the arc radius reflects the electrochemical process (*Rct*) and structural resistance of the electrode material. The *Rct* of CoO/C electrode is similar to that of other electrodes. The impedance comparison of three different samples shows that the introduction of C makes the material have a higher conductivity and can accelerate the electron transfer. The test results are employing the equivalent circuit embedded in Fig. 6. The R_1 represents the ohm resistance. CoO/C owns a R_1 value of 3.517Ω which is lower that of $NiCo_2O_4$ (15.4 Ω) and C (13.56 Ω). The R_2 values of CoO/C, $NiCo_2O_4$ and C are 2.29 Ω, 3.617 Ω and 2.472 Ω. CoO/C can reduce the resistance, accelerate the charge transfer, and thus increase the electrochemical reaction rate, which is in agreement with the previous description of CV curves. CPE is employed to compensate for the non-homogeneity of electrode materials, which illustrates the deviation of non-ideal capacitor. The CPE values of CoO/C, $NiCo_2O_4$ and C are 0.8723, 0.82848 and 0.84695. It implies that CoO/C contains a better capacitor behavior[25].

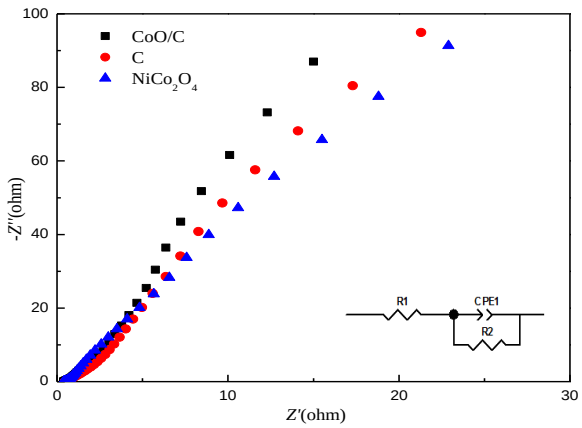

Figure 6. The electrochemical impedance spectroscopy of $NiCo_2O_4$, C and CoO/C in 6 M KOH

4. CONCLUSION

In conclusion, the needle-like CoO/C composite material was successfully constructed by a simple one-step hydrothermal method. Analysis of the structure and morphology suggest that CoO uniformly distributed in the composite and well combined with C. When used as a supercapacitor electrode, the CoO/C exhibited excellent electrochemical performance, with its specific capacitance reaching approximately 752 F/g in 6 M KOH aqueous solution. Moreover, in contrast to commonly carbon materials, the presented biomass carbon material for synthesizing CoO/C is simple, cost-effective and nonpolluting. The improved electrochemical performance shows that the synthesized CoO/C could be a promising material for a high capacity, low cost, and environmentally friendly material for supercapacitor.

ACKNOWLEDGEMENT
This work were supported by Postgraduate Research&Practice Innovation Program of Jiangsu Province (20820111950-SJCX19-0740) and (20820111964-SJCX19-0754), National Natural Science Foundation of China (grant no. 31800495), Natural Science Foundation of Jiangsu Province (grant no. BK20181040).

References

1. Q. Xie, A. Zheng, S. Zhai, S. Wu and Y. Guan, *J Solid State Electr.*, 20 (2015) 449.
2. Q. Sun, T. Jiang, G. Zhao and J. Shi, *Int. J. Electrochem. Sci.*, 14 (2019) 1.
3. H. Sun, X. Kong, B. Wang, S. Feng and G. Liu, *Int. J. Electrochem. Sci*., 14 (2019) 219.
4. M. Chen, Q. Zhou, X. Du, J. Zhang, W. Li, Y. Lu, D. Zhang, P. Qi and Y. Tang, *J Alloy Compd.*, 783 (2019) 363.
5. F. Lu, C. Zhang, J. Cheng, C. Zhu, H. Zhang and X. Cheng, *Int. J. Electrochem. Sci.*, 13 (2018) 9007.
6. C. Zhou, Y. Zhang, Y. Li and J. Liu, *Nano Lett.*, 13 (2013) 2078.
7. Z. Kai, L. Z. Li, X. S. Zhao and J. Wu, *Chem Mater.*, 22 (2010) 1392.
8. C. Liu, Z. Yu, D. Neff, A. Zhamu and B. Z. Jang, *Nano Lett.*, 10 (2010) 4863.
9. D. U. Xuan, C. Wang, M. Chen, Y. Jiao and J. Wang, *J Phys Chem C.*, 113 (2009) 2643.
10. A. Yuan and Q. Zhang, *Electrochem Commun.*, 8 (2006) 1173.
11. J. Jang, J. Bae, M. Choi and S. H. Yoon, *Carbon*, 43 (2005) 2730.
12. C. Kim and K. S. Yang, *Appl Phys Lett.*, 83 (2003) 1216.
13. C. Hai, B. Wei and M. A. Dongsheng, *IEEE T Power Electr.*, 25 (2010) 2897.
14. S. Hu, R. Rajamani and X. Yu, *Appl Phys Lett.*, 100 (2012) 4828.
15. W. C. Chen, T. C. Wen and H. Teng, *Electrochim Acta.*, 48 (2003) 641.
16. L. Pang, Z. Bo, H. Xue, L. Cao, W. Wei and Y. Guo, *Mater Lett.*, 184 (2016) 88.
17. M. Arulepp, J. Leis, M. Lätt, F. Miller, K. Rumma, E. Lust and A. F. Burke, *J Power Sources.*, 162 (2006) 1460.
18. J. Torop, V. Palmre, M. Arulepp, T. Sugino, K. Asaka and A. Aabloo, *Carbon*, 49 (2011) 3113.
19. D. Wei, L. Wei, Y. Sun, S. U. Qing and E. Xie, *Appl Surf Sci.*, 305 (2014) 433.
20. D. Wei, Y. Sun, Q. Su, E. Xie and L. Wei, *Mater Lett.*, 137 (2014) 124.
21. J. Deng, L. Kang, G. Bai, L. Ying, P. Li, X. Liu, Y. Yang, G. Feng and L. Wei, *Electrochim Acta.*, 132 (2014) 127.
22. G. Cao, J. Liu, C. Cheng, H. Li and J. F. Hong, *Energ Environ Sci.*, 4 (2011) 4496.
23. M. Pang, G. Long, J. Shang, J. Yuan, H. Wei, B. Wang, X. Liu, Y. Xi, D. Wang and F. Xu, *Chem Eng J.*, 280 (2015) 377.
24. Z. Ning, X. Yan, L. Jia, J. Ma and D. H. L. Ng, *Electrochim Acta.*, 226 (2017) 132.
25. Y. Xiao, A. Dai, X. Zhao, S. Wu, D. Su, X. Wang and S. Fang, *J Alloy Compd.*, 781 (2019) 1006.
26. G. Shen, W. Yao, B. Chen, K. Wang, K. Lee and Z. Lu, *IEEE T Power Electr.*, 29 (2014) 5542.
27. Y. G. Zhu, Y. Wang, Y. Shi, J. I. Wong and H. Y. Yang, *Nano Energy*, 3 (2014) 46.
28. P. Li, C. Ruan, J. Xu and Y. Xie, *J Alloy Compd.*, 791 (2019) 152.